

Weak localization in InSb thin films heavily doped with lead

M. Oszwaldowski* and T. Berus

*Institute of Physics, Poznań Technical University, Nieszawska 13a, 61-022 Poznań, Poland
and International Laboratory of High Magnetic Fields and Low Temperatures, Gajowicka 95, 53-529 Wrocław, Poland*

V. K. Dugaev

*Electronics and Communications Department, Instituto Superior de Engenharia de Lisboa,
Rua Conselheiro Emídio Navarro, P-1949-014 Lisbon, Portugal
and Institute for Materials Science Problems, Ukrainian Academy of Sciences, Vilde 5, 58001 Chernovtsy, Ukraine
(November 1, 2018)*

The paper reports on the investigations of the weak localization (WL) effects in 3D (about $2\ \mu\text{m}$ thick) polycrystalline thin films of InSb. The films are closely compensated showing the electron concentration $n > 10^{16}\ \text{cm}^{-3}$ at the total concentration of the donor and acceptor type structural defects $N_t > 10^{18}\ \text{cm}^{-3}$. Unless Pb-doped, the InSb films do not show any measurable or show very small WL effect at 4.2 K. The Pb-doping to the concentration of the order of $10^{18}\ \text{cm}^{-3}$ leads to pronounced WL effects below 7 K. In particular, a clearly manifested spin-orbit (SO) scattering is observed. That is ascribed to the large mass of the Pb atoms. From the comparison of the experimental data on temperature dependence of the magnetoresistivity (MR) and sample resistance with the WL theory, the temperature dependence of the phase destroying time τ_ϕ is determined. The determination is performed by fitting theoretical terms obtained from Kawabata's theory to experimental data on magnetoresistance. It is concluded that the dephasing process is connected to three separate interaction processes. The first is due to the SO scatterings and is characterized by temperature-independent relaxation time $\tau_{so} \simeq 10^{-12}$ s. The second is associated with the electron-phonon interaction ($\tau_i \sim T^{-3}$). The third dephasing process is characterized by independent on temperature relaxation time $\tau_c = (1\ \text{to}\ 7) \times 10^{-12}$ s. This relaxation time is tentatively ascribed to inelastic scattering at extended structural defects, like grain boundaries. The resulting time τ_ϕ shows saturation in its temperature dependence for $T \rightarrow 0$. The temperature dependence of the resistance of the InSb<Pb> films can be explained by the electron-electron interaction for $T < 1$ K, and by the WL effect for $T > 2$ K.

PACS numbers 73.20.Fz; 72.15.Rn; 72.10.Fk.

I. INTRODUCTION

Because of its unique physical properties InSb is one of the most interesting materials for the investigation of the weak localization (WL) effects. The critical electron concentration n_{cr} for the metal-insulator transition (MIT) in InSb is about $10^{14}\ \text{cm}^{-3}$, which is the smallest value among semiconductors.¹ This small critical concentration results in a metallic conduction that can be realized with the help of donor doping, in the electron concentration range that spans over five orders of magnitude. This peculiar property allows the realization of various physical situations under which the localization effects can be investigated and compared with the existing theories. For the impurity concentrations below $10^{19}\ \text{cm}^{-3}$, the Γ conduction band structure is not disturbed meaningfully and hence in the interpretation of the experimental data the known material parameters of structurally perfect InSb can be exploited.

Among those parameters the most important for the effect in question is the small effective mass at the bottom of conduction band, $m^* = 0.014 m_e$ (m_e is the free electron mass) and high electron mobility which is very sensitive to the presence of structural defects. The small electron effective mass corresponds to a low density of

states at the bottom of the conduction band. In such case, even at relatively low electron density, the condition of applicability of the WL theory, $E_F\tau/\hbar \gg 1$, is fulfilled (E_F is the Fermi energy and τ is the elastic scattering time).

The small effective mass in conjunction with a large static dielectric constant, $\epsilon_s = 17.5$, causes that the effective Bohr radius a_B^* is very large, $a_B^* = \epsilon_s \hbar^2 / m^* e^2 \simeq 73$ nm. As a consequence, the non-ideality parameter, which determines a relative importance of the interaction effect, $k_F a_B^* \simeq 4k_F^2 \lambda^2$ is large for $n > n_{cr}$ (λ is the screening length). In such a case the corrections from interaction become smaller than those from localization. We estimate that the transition from interaction to localization occurs in the electron concentration range $10^{14} - 10^{15}\ \text{cm}^{-3}$.

In spite of those particular advantages as offers the metallic InSb, only several investigation teams studied the WL effects in this semiconductor.²⁻⁵ In all papers, bulk crystals of InSb with electron concentrations $n < 5 \times 10^{15}\ \text{cm}^{-3}$ were investigated. The studies revealed a divergence in the interpretation if the corrections are related to localization or electron-electron interactions. The WL effects were observed at temperatures smaller than 1 K and their strength was smaller than that per-

dicted by the theory.

In the present paper we investigate the WL effects in three-dimensional (3D) polycrystalline thin films of InSb heavily doped with electrically neutral lead. The background effective donor concentration in these films is between $1.6 \times 10^{16} \text{ cm}^{-3}$ and $2 \times 10^{17} \text{ cm}^{-3}$, which means that we investigate samples with much higher concentration than in previous studies. Hence, we expect that for the present concentrations the corrections should be related mostly to localization effects. Note that the results of Ref. [3] have demonstrated that the corrections are due to the interaction.

In our samples of InSb<Pb> films, the WL effect is observed at relatively high temperatures, $T \leq 7 \text{ K}$ and is also much more pronounced in the magnetoresistance (MR) as compared to the earlier observations. A particular feature of the samples is a clearly marked effect of the SO interaction (positive MR) at the lowest magnetic fields. The SO scattering was not observed in the previous investigations performed on InSb doped with shallow donors. The presently observed SO interaction seems to be associated with the doping with Pb, and in such a case is due to its large atomic number. The enhancement of the WL in InSb<Pb> films can be ascribed to the scattering of electrons from short-range potentials of Pb atoms incorporated substitutionally into the InSb lattice in pairs for neighboring In-Sb pairs (we discuss it in Sec. III).

For the interpretation of our experimental results we had to complete the commonly accepted formulae for the WL corrections⁶⁻⁸ to take into account the specific features of InSb. They are a strong SO interaction and a strong Zeeman splitting of spin up and down electrons in magnetic field (Landé factor for InSb is $g = -51.3$). These effects have been discussed separately in Refs. [10-13]. In particular, in a theoretical work of Isawa et al.,¹³ dedicated to the localization and interaction effects in InSb, only Zeeman splitting has been taken into account, whilst SO coupling has not. Since our MR experiments show the importance of SO coupling, we have to make necessary generalizations of the known formulas to take into account both SO scattering and Zeeman splitting.

The investigation of the WL effects have acquired a new impact in recent years. This is, to a great extent, due to the problem of the temperature dependence of the electron dephasing time (for a quick introduction of the problem and relevant literature consult Ref. [14]). Our paper is also relevant to this problem.

The paper is arranged as follows. In Section II we describe the preparation method of InSb films and their doping with Pb. Section III is devoted to the interpretation of the inherent electrical properties of the InSb films, which are associated with the presence of electrically charged structural defects and their non-uniform spatial distribution. In Section IV we discuss the WL effects observed below 7 K. Section V summarizes our finding and conclusions.

II. SAMPLE PREPARATION AND CHARACTERIZATION

Thin films of InSb for the present investigations were obtained by the flash evaporation method. High purity (zone refined) InSb with the net donor concentration $N_d - N_a < 5 \times 10^{15} \text{ cm}^{-3}$ was used for the evaporation. The films were evaporated on ceramic substrates through mechanical masks and were shaped for conductivity and Hall effect measurements. They have thickness of about $2 \mu\text{m}$. Details of these experimental procedures are given elsewhere.¹⁵

The obtained polycrystalline InSb films have rather typical properties for the given preparation conditions. Such films have electrical properties governed by their structural defects.¹⁶ Without any intentional doping the films are of *n*-type. With the increase in substrate temperature the number of structural defects decreases and the electron concentration decreases, whilst the electron mobility increases. The mobility is also dependent on film thickness: below $3 \mu\text{m}$ it markedly decreases with the film thickness. In the thicker films obtained at substrate temperatures $T_s \geq 450^\circ\text{C}$, the lowest electron concentration is of about $2 \times 10^{16} \text{ cm}^{-3}$, and the highest room temperature electron mobility is in excess to $10000 \text{ cm}^2/\text{V}\cdot\text{s}$. For this electron concentration the mobility is a half-of-order magnitude smaller than that in uncompensated bulk crystals of InSb. The large number of structural defects of the donor and acceptor type, which partly compensate each other, can explain this mobility drop. Below room temperature the mobility decreases with temperature, which can be explained by the barrier mechanism (see Sec. III).

Lead doping was performed by the co-evaporation of InSb and Pb from separate evaporation sources. This procedure was essentially the same as that used for doping of InSb films with tin.¹⁷ The lead doping, up to the solubility limit, which is of the order of 0.02 atomic percents ($3 \times 10^{18} \text{ cm}^{-3}$), has no electrical influence on the doped InSb films, except for the lowest temperatures. We explained this electrical neutrality of lead by a particular incorporation into the InSb lattice.¹⁷ Lead is an amphoteric impurity in InSb and incorporates to the InSb matrix in pairs substituting the neighbor pairs In-Sb. In this sense Pb is an isoelectronic impurity in InSb. However, in our samples the solubility limit is overrun and in result the InSb<Pb> films have microscopic inclusions of lead. Detailed investigations suggest^{17,18} that a part of those inclusions can transit to superconductivity below 5 K.

We investigate four samples of InSb<Pb>: samples 732, 725A and 725B, obtained at $T_s = 370^\circ\text{C}$, and sample 727, obtained at $T_s = 340^\circ\text{C}$. Their basic electrical parameters, as obtained by the Hall measurements at 4.2 K, are given in Table 1. Samples 725A and 725B were

obtained at the same evaporation run and their electrical parameters are very similar. For this reason in Table 1 we present only the parameters of sample 725B.

In Table 1, d is the thickness of InSb film, μ is the electron mobility and n is the electron concentration. The meaning of other parameters is explained in Sec. III.

The dependence of resistivity of all InSb<Pb> films on temperature and magnetic field is of the same character, but is different in details. In Fig. 1 we present results for samples 725B and 727 below room temperature. These temperature dependences are typical for polycrystalline InSb thin films, except the low temperature region below 7 K. The sharp resistivity increase with the temperature decrease in this region, shown in the inserts, was observed only in Pb-doped InSb films. We ascribe this low-temperature increase in resistivity to the WL effect (see Sec. IV,B). It is worth noting that the transition to the localization does not always have such an abrupt form as those seen in the inserts. For example, this transition for sample 725A has a smoother form.

In the considered temperature range, the electron density in the InSb films is independent of temperature, if we neglect a small decrease in the vicinity of room temperature. Thus, the increase in resistivity is solely due to a decrease in the mobility. This decrease in mobility as well as the stronger temperature dependence of the mobility in samples with smaller electron concentrations is rather typical for polycrystalline InSb thin films.^{15,16}

The transversal and longitudinal magnetoresistivity of the samples at 4.2 K is presented in Fig. 2. The observed MR, except for the low field region shown in the insert, is also typical for InSb films. The negative MR in the low field region is characteristic for Pb-doped InSb films. Actually, in a narrow temperature range, and in magnetic fields below 0.1 T, the MR is positive (Fig. 3), but in the course of measurements shown in Fig. 2, this region has not been traced and for this reason the positive MR does not appear in the figure.

The sample investigations in the temperature range 1.7 to 295 K have been performed at the International Laboratory of High Magnetic Fields and Low Temperatures in Wroclaw, and the investigations in the temperature range 0.04 to 2 K have been carried out at the Institute of Low Temperatures and Structural Investigations in Wroclaw, Poland.

III. INTERPRETATION OF ELECTRICAL PROPERTIES OF InSb FILMS AND EFFECT OF Pb DOPING

As mentioned above, the dependence of sample resistance on temperature or magnetic field, except for the lowest temperature and fields, is substantially the same in InSb films doped and undoped with Pb. The low temperature effects below 7 K, recognized as the WL, will be discussed in Sec. IV. First we discuss the properties,

which are common for InSb and InSb<Pb> films, and then we consider the role of Pb doping.

The temperature dependence of the resistivity of polycrystalline InSb thin films down to 7 K can be explained by a large concentration of electrically active structural defects that scatter electrons. These defects are impurities and other point defects, such as interstitials, vacancies, stacking faults, etc. If a possible non-uniformity in the distribution of the ionized defects is ignored, the low temperature mobility can be described by the Brooks-Herring formula that takes into account the conduction band non-parabolicity of InSb.¹⁹ For an electron concentration n , the formula gives the following mobility in a compensated sample:

$$\mu_i = \mu_{io}(n) \frac{n}{n + 2N_a}, \quad (1)$$

where $\mu_{io}(n)$ is the electron mobility limited by the ionized impurities in an uncompensated sample, and N_a is the concentration of acceptors. For $\mu_{io}(n)$ we use the experimental data, instead of the theoretical ones, to avoid the question about the validity of the classical theory at very low temperatures.

Consider InSb<Pb> thin film with a typical electron concentration of $2 \times 10^{17} \text{ cm}^{-3}$ and mobility $\mu = 1000 \text{ cm}^2/\text{V}\cdot\text{s}$. For this concentration, a low temperature $\mu_{io}(n)$ is $(4 \text{ to } 5) \times 10^4 \text{ cm}^2/\text{V}\cdot\text{s}$.²⁰ Inserting this value into Eq. (1), one obtains the acceptor concentration $N_a \geq 4 \times 10^{18} \text{ cm}^{-3}$. This value seems to be too high, as the resulting high degree of compensation $K = 0.95$ is rather improbable for an accidental compensation process. Hence, we assume that the small mobility is only partly due to the compensation effect.

Since InSb has an isotropic conduction band, any classic longitudinal MR should not be observed. Also the magnitude of the positive transversal MR is higher than that expected for uniformly doped InSb having the same electron concentration. The observed longitudinal MR as well as the relatively large transversal MR have to be associated with a non-uniform distribution of the charged defects. These effects of non-uniform distribution have been predicted by Herring.²¹ However, assuming reasonable fluctuations of the electron density, the theory predicts much smaller longitudinal MR than we observe. In order to explain the observed effects, we assume that the polycrystalline InSb thin films show not only a large number of defects of the donor and acceptor type but also that their compensation degree fluctuates strongly. Such fluctuations can for example be generated at grain boundaries.

With this assumption we can adopt to our samples the explanation of the galvanomagnetic properties of compensated bulk n -InSb proposed by Aronzon et al.⁵ In n -InSb, due to the low density of states and high dielectric constant, the compensation fluctuations can create macroscopic potential fluctuations. In result, the electrons are located in potential wells separated by some potential barriers. Thus, the electric conduction takes

place in a material composed of macroscopic areas of a metal-like phase separated by regions of an insulating phase. The conduction is of percolating character and can be described by a percolation level E_p . At $T = 0$ the conduction can take place only when the Fermi level $E_F > E_p$.

In this model, the measured macroscopic mobility is thermally activated and hence the resistivity decreases with increasing temperature. At low temperatures, the microscopic mobility (we define the microscopic mobility as that inside the potential wells) also decreases with temperature as it is mostly limited by the scattering from charged defects. However, the macroscopic mobility, measured in the Hall experiments, is mainly limited by the percolation. In such a case the current lines are of zigzag shape, and in result the measured MR has both the transversal and longitudinal component. Therefore, the assumed percolative conduction model explains both the temperature dependence and magnetic field dependence of the sample resistivity, shown in Figs. 1 and 2, respectively.

For small values of $E_F - E_p$, i.e. closer to the MIT of the percolative type, the temperature and field dependence of the resistivity should be stronger. Closer to the MIT are the samples with smaller electron concentration. As is seen in Figs. 1 and 2, sample 725B having smaller n shows stronger dependencies of $\rho(T)$ and $\rho(B)$ indeed.

We now examine the low-temperature region where the WL effects occur. Since pronounced localization effects take place only in samples doped with Pb, we also have to consider a possible effect of Pb-doping on both elastic τ and inelastic τ_φ relaxation times (here τ is defined as the microscopic magnitude). When τ changes due to the doping with Pb, the macroscopic mobility does not change substantially since it is mainly limited by the percolation. Therefore, in frame of this model, we do not rule out a decrease in the microscopic mobility due to Pb doping. However, this decrease can not cause any dramatic changes in the WL observation, because the WL correction in 3D case depends on the relaxation time as $\sqrt{\tau}$.^{6,7} We believe that to understand the role of Pb doping, it is important to take into account that the neutral Pb atoms interact with electrons by short-range potentials, like strongly screened ionized impurities in metals. Large number of such defects creates necessary conditions for diffusive motion of electrons, which results in the WL effect. The suggestion that the WL is related to the electron scatterings on Pb atoms can further be confirmed by the discussed in Sec. IV antilocalization effect due to the SO interaction. According to the theory,²⁴ the SO scattering depends on the impurity atom mass as Z^4 . More recent theoretical results for Mn suggest that the dependence be as Z^2 and the scattering can also depend on the impurity valency.²⁵ Thus, both the theories predict strong SO scattering from heavy impurities. It should be mentioned that in previous studies performed on InSb crystals²⁻⁵ no SO effects have been observed.

In principle, there is a possibility that the Pb dop-

ing increases the inelastic relaxation time associated with the electron-phonon interaction, by changing the phonon density of states. It would increase the localization corrections.^{6,7} However, this possibility should be ruled out because the corresponding changes in the low-energy phonon spectrum turn out to be too small to change meaningfully the relaxation time τ_φ . Besides, the Pb doping should rather decrease than increase the inelastic relaxation time because heavy impurities usually increase the phonon density of states on the low energy side.²²

IV. WEAK LOCALIZATION EFFECTS

The important parameters of our samples from the viewpoint of the WL are given in columns 5-9 of Table 1. The values of parameters estimated from the Hall measurements at $T \simeq 7$ K are presented without parentheses. There v_F is the electron Fermi velocity, k_F is the Fermi wavevector, and l is the mean free path of electrons. The physical meaning of other parameters is the following. $1/k_F l$ is a basic parameter of the WL theory. The WL theory works for $(1/k_F l) \ll 1$. r_s is the interaction parameter. Interaction is expected to be less important if $r_s \ll 1$. B_c is a critical field in Kawabata's theory of magnetoconductivity.²⁶ For $B > B_c$ the localization corrections are suppressed completely by the magnetic field. $l_\varphi = (D\tau_\varphi)^{1/2}$ is the dephasing mean free path. $D = v_F l/3$ is the diffusion constant in 3D case. For the estimation of l_φ we assume $\tau_\varphi = 10^{-12}$ s at 4.2 K. The detailed analysis (see Sec. III,A) confirms this value.

From Table 1 one can conclude the following. The condition of effective three-dimensionality,^{10,7} $l_\varphi \ll d$, is fulfilled in all our films. However, for sample 732 the condition $1/k_F l \ll 1$ is not fulfilled. This means that for that sample the WL theory might not be applicable. Also, for this sample the magnetic freezing critical field (see below) turns out to be lower than for the other samples. However, even in this case the magnetic freezeout is not likely to occur.

In the magnetic field region of interest, $B < 0.3$ T, the classical magnetoconductivity of the samples is expected to be negligible. This is because in this magnetic field region the condition of classically weak magnetic fields, $\mu B \ll 1$, is fulfilled for all samples.

In all studied samples the condition $l \ll a_B$ is fulfilled. This condition is important from the point of view of applicability of the interaction theory in its usual form.^{6,8} Our estimations show that the inequality $l \ll a_B$ can change the temperature dependence of resistivity at $\hbar/\tau < kT < E_F l/a_B$.

In the case of InSb a question of the critical field for the magnetic freezeout of electrons at impurities may be risen. This magnetic field can be estimated from the relation $n(a_B l_B^2)^{1/3} \simeq 0.34$,³ where $l_B = (\hbar/eB)^{1/2}$ is the magnetic length. In our samples, such a critical field is

higher than 2 T, and thus the freezeout does not take place at the fields in question.

A. Magnetoresistance

In all samples the dependence of resistivity on magnetic field for $B < 0.3$ T and $T < 7$ K, is such that it first increases and then decreases with magnetic field. A typical example of this behaviour is shown in Fig. 3. The shown experimental data on magnetoresistance are related to the WL effect exclusively. A small contribution to the magnetoresistance from the classical (Lorentz) effect is subtracted on the basis of the extrapolation of the classical magnetoresistance from the higher magnetic

fields (Fig. 2).

The clearly seen positive MR region at the lowest magnetic fields can be explained within the WL theory as the result of strong SO scattering.^{9,10} The negative MR, seen at magnetic fields higher than 0.05 T is the normal behavior expected for the case of weak localization when the SO interaction (the antilocalization) can be neglected.

In order to perform theoretical curve fitting to the experimental points, with the aim of determination of the sample parameters, we adopt the usual Kawabata's approach to the magnetoresistivity in 3D case.²⁶ The original formulae for the conductivity corrections have to be generalized to take into account both SO coupling and Zeeman splitting. We find that the contribution from singlet Cooperon that contains Zeeman splitting is

$$\Delta\sigma_s(B) - \Delta\sigma_s(0) = \frac{e^2}{4\pi^2\hbar l_B} \sum_{n=0}^{\infty} \left\{ \frac{\cos(\varphi_1/2)}{\left[(n+1/2+\delta)^2 + \nu^2\right]^{1/4}} - 2\cos(\varphi_2/2) \left[(n+1+\delta)^2 + \nu^2\right]^{1/4} + 2\cos(\varphi_0/2) \left[(n+\delta)^2 + \nu^2\right]^{1/4} \right\} \quad (2)$$

and that from triplet Cooperon, which contains SO scattering is

$$\Delta\sigma_t(B) - \Delta\sigma_t(0) = -\frac{3e^2}{4\pi^2\hbar l_B} \sum_{n=0}^{\infty} \left[\frac{1}{\sqrt{n+1/2+\delta_{so}}} - 2\left(\sqrt{n+1+\delta_{so}} - \sqrt{n+\delta_{so}}\right) \right]. \quad (3)$$

Here we denoted: $\delta = l_B^2/4D\tau_\varphi$, $\delta_{so} = (l_B^2/4D)(1/\tau_\varphi + 4/3\tau_{so})$, $\nu = g\mu_B/4eD$, $\varphi_0 = \arctan[\nu/(n+\delta)]$, $\varphi_1 = \arctan[\nu/(n+1/2+\delta)]$, $\varphi_2 = \arctan[\nu/(n+1+\delta)]$, and μ_B is the Bohr magneton.

For shortness we imply here τ_φ is the total phase relaxation time. The total localization correction to conductivity is the sum of (2) and (3).

We used Eqs. (2) and (3) for the fitting of theoretical curves to the experimental dependence of the magnetoresistivity $\rho(B)/\rho(0)$ at low magnetic fields and various temperatures. In the calculations we take the measured conductivity $\sigma = \sigma_0 + \Delta\sigma$, where $\sigma_0 = en\mu$ is the classical conductivity, which we assumed to be independent upon magnetic field in the field region in question.

To fit the magnetoresistivity curves we had to choose four parameters τ_φ , τ_{so} , n and μ and their temperature dependencies. The last two parameters determine the Fermi velocity and the elastic relaxation time. We have assumed that n is temperature independent and μ is weakly dependent on temperature in the temperature range in question. So, the observed weak temperature dependence of the samples resistance is solely due to the weak temperature dependence of the mobility. We have also assumed that τ_{so} is independent of temperature. This results from the assumed temperature inde-

pendence of the SO interaction and the elastic electron free path. Such an assumption is frequently adopted.²⁷

An example of the theoretical curve fitting to experimental points obtained for sample 727 is shown in Fig. 3. As is seen, a good agreement between experiment and theory is reached only at the lowest magnetic fields. This is acceptable, as Eqs. (2) and (3) hold only for the lowest magnetic fields.¹³

Sample parameters, obtained from the curve fittings, are given in Table 1 in parentheses. They can be compared to those obtained from the Hall measurements. In our attempts to fit the theoretical curves to the experimental data we found it impossible to reach the values of concentration and mobility obtained from the Hall measurements. In the case of sample 732 we found an increase in the mobility by a factor of about 3. This means that the microscopic mobility in this sample, as expected, is considerably higher than the macroscopic one. With this higher microscopic mobility, the condition $1/k_F l < 1$ is fulfilled, which confirms the applicability of the WL theory to the description of the magnetoresistivity.

In the case of samples 725 and 727 we found a relatively small increase in the mobility along with a considerable decrease in the electron concentration. The origin of this discrepancy is not quite clear. We can suppose that the

Hall measurements were influenced by the Pb inclusions. Due to a possible short-circuiting effects on the Hall voltage, the determined electron concentration can be higher than the microscopic one.

In our curve fitting to the magnetoresistance measured at different temperatures, we have assumed that the theoretical description has to use the same set of material parameters τ_{so} , n , and μ . This assumption appeared to be very restrictive and resulted in a considerable uncertainty in the determination of τ_φ (see Fig. 4). Moreover, to obtain improved fits we were forced to introduce into $\Delta\sigma$ a temperature-dependent prefactor $\alpha(T)$. The value of α at $T = 4.2$ K is 1.0 for sample 732, 0.90 for sample 727, and 0.94 for sample 725B. The value of $\alpha(T)$ at $T = 0.68$ K is 0.87 for sample 732 and 0.76 for sample 727. Sample 725B has not been measured at 0.68 K, but at $T = 1.8$ K it has $\alpha = 0.81$. Therefore, the prefactor introduces small corrections to the calculated curves mainly at the lowest temperatures.

It should be mentioned that in previous papers devoted to the WL effect in InSb^{2,3,5} a prefactor of a constant value was also introduced because the magnitude of the experimental magnetoresistance was always smaller than that predicted by the theory. The value of the prefactor was in the range $\alpha = 0.02 - 0.55$. In the present case there is no problem with the magnitude of the effect, but with its temperature dependence. The temperature dependence of $\alpha(T)$ seems to be correlated with the dose of Pb obtained by a given sample. The doses obtained by samples 725 and 727 were higher than that obtained by sample 732. We think that the temperature dependence of α can be related to this part of Pb inclusions that can transit to superconductivity. The effect of the superconducting inclusions on the sample magnetoresistance was discussed in Ref. [17].

The high concentration of Pb in the InSb films may suggest that the contribution of the superconducting fluctuations, known as Maki-Thompson corrections,²⁹ can play a significant role in the temperature dependence of the conductivity. The Maki-Thompson corrections change $\Delta\sigma$ by a factor $\beta(T)$ such that $0 \leq \beta(T) \leq 1$. This factor is related to $\alpha(T)$ as $\alpha(T) = 1 - \beta(T)$. However, the temperature dependence of α in sample 727 can hardly be explained by Maki-Thompson corrections because the corrections are rather smaller and have different temperature dependence.

The temperature dependence of τ_φ and τ_{so} for the four samples obtained from the fittings are presented in Fig. 4. The bars attached to the values of τ_φ show the ranges where the curve fitting is still reasonable, with the other parameters kept constant.

As is seen, the obtained SO relaxation time is nearly the same in all samples and it is about $\tau_{so} = 1.2 \times 10^{-12}$ s. We can not compare this value with any earlier data, because, as far as we know, these are the first data on the SO scattering from impurities in conduction band of a 3D semiconductor sample. Thus, we compare the scattering time with the data for 2D metallic films covered with

about a monolayer of impurities compiled in Ref. [30]. For the heaviest impurity atoms a value of $\tau_{so} \leq 10^{-12}$ s is characteristic, which is close to our value. It is believed that the probability of SO scattering is proportional to the atomic number of the impurity and the inverse of the elastic relaxation time. However, a detailed value is determined by the relevant conduction band parameters.³⁰ Thus, the relaxation times τ_{so} in our samples should be proportional to the electron mobility. Actually, such correlation in our samples is not observed. This can be explained by a difference in the Pb concentrations between different samples. Such a dependence of τ_{so} on the heavy impurity concentration was observed in Mg films doped with Bi.²⁷

As is seen in Fig. 4, at 4.2 K, τ_φ for all samples is of the order of 10^{-12} s, and thus is close to the value of τ_{so} . However, the most striking feature of τ_φ is its weak temperature dependence, when compared with earlier investigation results. It should be pointed out that usually a dependence of the form

$$\tau_\varphi^{-1} \sim T^p \quad (4)$$

is assumed for the inelastic processes. In particular, $p = 2$ for the electron-electron interaction and $p = 3$ for the electron-phonon interaction in the clean limit.^{10,32,33}

Dynes et al.² found that in their samples $\tau_\varphi \sim T^{-3}$ in the temperature range 0.05 to 1.5 K. Extrapolating this dependence in Fig. 3 of Ref. [2] to 4.2 K, one obtains $\tau_\varphi = 1.3 \times 10^{-12}$ s, a value close to our result. On the other hand, Mani et al.⁴ obtained for the temperature range 0.5 to 4.2 K, $\tau_\varphi \sim T^{-2}$, with $\tau_\varphi = 4 \times 10^{-12}$ s at 4.2 K.

It should be mentioned that the saturation of τ_φ at low temperatures has been observed earlier many times at lowest temperatures, and it had been usually attributed to the effect of magnetic impurities.^{9,34} This mechanism can not, however, be responsible for the presently observed saturation of τ_φ . This is because in our samples important could be only magnetic impurities in concentration $> 10^{17}$ cm⁻³. Such a large uncontrolled doping should be ruled out from the point of view of our technology of the sample preparation. Moreover, the solubility limits of the typical magnetic impurities Fe, Co, Ni in InSb is below 10^{14} cm⁻³.³⁵

The saturation of τ_φ in InSb<Pb> films has been earlier demonstrated in Ref. [36]. Meantime we performed further experimental studies of the MR effect and we gathered further evidence for the saturation. In these experiments we have paid a particular attention to the possible thermal effect connected to the sample driving current. We are convinced that the presented here saturation effect is not a result of the current heating.

The saturation of τ_φ at low temperatures and in the absence of magnetic impurities has been recently reported^{37,38} and critically discussed in theoretical papers.³⁹⁻⁴¹ While the existence of the saturation is still a subject of controversy, it seems to emerge that an explanation of the observed weak temperature dependence

of τ_φ in some disordered metals is an additional independent on temperature relaxation mechanism. A simple example of such a mechanism is the inelastic scattering from two-level centers.^{14,42} In our case we can assume that this mechanism is associated with inelastic interactions of the conducting electrons in the course of their transmission through potential barriers located at extended structural defects like grain boundaries. We can expect the presence of dangling bonds, acting as two-level centers, in the vicinity of the grain boundaries. In this case, we should make the following substitution in the relevant equations

$$\tau_\varphi^{-1} = \tau_i^{-1} + \tau_c^{-1}, \quad (5)$$

where τ_i is the inelastic relaxation time related to intrinsic mechanisms of relaxation that characterises uncompensated bulk InSb and τ_c is an independent on temperature relaxation time, which can be related to the potential well of radius L_c , $\tau_c = L_c^2/D$.

Assuming that τ_i is of the form of Eq. (4) with p being an integer, the best fit of the relation (5) to the points in Fig. 4 is obtained for $p = 3$. The solid curves in the figure are calculated from Eq. (5) with

$$\tau_i = 1.95 \left(\frac{4.2}{T} \right)^3 10^{-12} [s]. \quad (6)$$

The values of τ_c used in the calculations can be read out from Fig. 4 as the values of τ_φ at $T = 0$. The dependence of the type of Eq. (6) represents the electron-phonon relaxation mechanism in pure metals. The fact that the same dependence of Eq. (6) can be used for the calculations of all the curves is a further confirmation of relaxation time mechanism, because the electron-phonon interaction is independent on the electrical properties of the sample.

In pure metals, for $kT \gg \hbar c_l/l$, the electron-phonon relaxation time can be calculated using the formula^{32,33}

$$\frac{1}{\tau_{e-ph}} = \frac{7\pi}{10} \frac{(k_B T)^3}{\hbar m M c_l^4}, \quad (7)$$

where m and M respectively are the electron and ionic masses, and c_l is the longitudinal phonon velocity. Assuming for InSb $c_l = 3.8 \times 10^3$ cm/s to be an averaged over crystallographic directions sound velocity,⁴³ we find that for the samples investigated the condition $kT \gg \hbar c_l/l$ is fulfilled for $T > 2.4$ K. If we assume that in the case of semiconductors the electron mass in Eq. (7) is the effective mass m^* , then for InSb at 4.2 K we obtain $\tau_{e-ph} = 5 \times 10^{-11}$ s. This value is by a factor of 25 higher than that obtained from our experiments. Such discrepancy is however expected taking into account the fine crystalline character of our samples. First, we expect that c_l in our samples is smaller than in InSb single crystal. Secondly, Eq. (7) assumes that the longitudinal and transversal phonon velocities are approximately equal, $c_l \simeq c_t$ (in cubic crystals $c_l \simeq \sqrt{3}c_t$), and in such a case

the transversal phonons can be neglected. In strongly defected samples c_t can be considerably more reduced than c_l . In such a case the transversal phonons can be important, which means that that the $e-ph$ relaxation time is further reduced.

B. Temperature dependence of resistance

The temperature dependence of the samples resistance between 0.04 K and 7 K is displayed in Fig. 5. These dependencies are interpreted using the WL theory, taking into account both localization and interaction corrections.

The localization correction to the conductivity at three dimensions ($d = 3$), which includes SO coupling, can be obtained by a generalization of the formula of Ref. 6 to the form:

$$\delta\sigma_{loc} = \text{const} + \frac{e^2}{4\pi^2\hbar\sqrt{D}} \left[3 \left(\frac{1}{\tau_\varphi} + \frac{4}{3\tau_{so}} \right)^{1/2} - \left(\frac{1}{\tau_\varphi} \right)^{1/2} \right]. \quad (8)$$

The interaction correction is

$$\delta\sigma_{int} = \text{const}_1 + 2.5 \frac{\sqrt{2} e^2 T^{1/2}}{6\pi^2 \hbar D^{1/2}}. \quad (9)$$

Here we take into account only the exchange diagram contribution,⁶ and do not consider the Maki-Thompson corrections. It makes sense for the weak electron-electron interaction, when $k_F\lambda \gg 1$.

In general, the resistance below 1 K exhibits a dependence of the type $R \sim T^{-1/2}$. This dependence is shown by dashed lines in Fig. 5. Therefore, the electron-electron interaction is responsible for the temperature dependence in this temperature region. The exception from the rule is sample 727 that shows a maximum in its temperature dependence. We ascribe this anomaly to the superconducting Pb inclusions, which can decrease the resistance.

At higher temperatures, the temperature dependence of the samples resistance can be described by Eq. (8), in which the temperature dependence of τ_φ is given by the solid curves in Fig. 4. The dependence $R(T)$ is shown in Fig. 5 by the solid lines. As is seen, between 2 K and 5 K the character of the temperature dependence of the samples resistance is well approximated by the calculated curves. Above 6 K the quantum corrections to the resistance can be neglected. We draw attention to the fact that both the magnetoresistivity at various temperatures and the temperature dependence of the samples resistance can be explained with the help of the same temperature dependence of τ_φ given by Eq. (5), in which an important role plays the temperature independent relaxation time τ_c .

Sometimes one argues that the saturation of τ_φ is an artifact associated with the warming effect of the sample driving current (see the discussion in Ref. [38]). In this

connection we wish to point out the fact that in Fig. 5 the resistance sharply increases with decreasing temperature in the low temperature region where the dephasing time saturates. This confirms that the hot-electron effects due to Joule heating do not take place. If Joule heating occurred, the temperature dependence of the resistance would saturate.

V. SUMMARY AND CONCLUSIONS

This paper reports on the first observation and analysis of the weak localization effects in 3D InSb thin films heavily doped with lead. The investigated InSb<Pb> films are prepared by vacuum coevaporation of high purity In, Sb and Pb from separate evaporation sources. They are of polycrystalline nature and show the electron concentration $n > 10^{16} \text{ cm}^{-3}$, which is independent on temperature in the low temperature region (the metallic behavior). This concentration is equal to the net donor concentration, and it is due to the structural defects. The total number of donor and acceptor type structural defects is estimated for $> 10^{18} \text{ cm}^{-3}$. Thus, the presently investigated samples of InSb are closely compensated and have both the electron and total defect concentrations considerably higher than those in the reported previous investigations.

The concentration of lead atoms incorporated into the crystal lattice is estimated to be also of the order of 10^{18} cm^{-3} . This concentration corresponds to the solubility limit of Pb in InSb. Lead incorporates into the lattice of InSb mainly in pairs substituting for neighboring In-Sb pairs. In this sense it is an isoelectronic impurity that is electrically neutral (it does not supply mobile carriers). The predominant lattice incorporation in pairs is concluded from the experimental fact that at the given background of electrically active defects the Pb-doping do not appreciably change neither the electron concentration nor the mobility of the doped films.^{17,18}

From the thermally activated resistivity observed below room temperature (Fig. 1) and the large longitudinal magnetoresistivity (Fig. 2), a percolative mechanism of electrical conduction is gathered. In this conduction model, electrons are located in potential wells separated by potential barriers. These potential fluctuations can be related to the extended structural defects like dislocations, growth flaws, grain boundaries, etc, as well as to the compensation degree fluctuations related to the point defects. Within such a model one can expect the macroscopic percolative electron mobility (the one measured in the Hall experiments) is smaller than the microscopic one, limited by the ionized defects scattering only. This expectation is confirmed by the present experiments. Namely, in order to fit the theoretical curves for magnetoresistivity (MR) obtained in the frame of the WL theory, to experimental points, we have to assume that the microscopic mobility is higher (see Table 1).

Doping of InSb films with Pb results in pronounced WL effects: at temperatures lower than 7 K, the resistance rapidly increases (Fig. 1). The effect magnitude and temperature range is considerably higher than those observed previously in pure InSb.²⁻⁴ The relation of the WL effect to the presence of Pb impurities seems to be further confirmed by the positive magnetoresistance observed at the lowest magnetic fields (Fig. 3), which is apparently due to the SO scattering. This effect clearly demonstrates that the electrons are scattered from heavy atoms. In the previous investigations only negative MR was observed (no SO interaction has been found). As far as we know, this is the first observation of SO scattering of electrons in the conduction band of a 3D semiconductor sample.

However, it is not quite clear in which way the doping with lead could enhance the WL effect. We suggest that it can be associated with short-range potentials of the substitutionally incorporated Pb atoms. This problem has to be clarified in further studies.

To interpret the low temperature MR in our samples, we had to adopt the theoretical expressions of Kawabata²⁶ to the particular case of InSb. We generalized the formulae to take into account both SO coupling and Zeeman splitting, Eqs. (2) and (3). From the curve fitting we obtained the SO dephasing time $\tau_{so} \simeq 10^{-12} \text{ s}$. This appears to be a reasonable value for scatterings on heavy atoms like Pb.

The fitting also supplied the temperature dependence of the phase relaxation time τ_φ shown in Fig. 4. A particular feature of that dependence is saturation for $T \rightarrow 0$. We show that this peculiar temperature dependence can be explained if one assumes that τ_φ is a combination of two inelastic relaxation times τ_i and τ_c (Eq. (5)). The inelastic relaxation τ_i given by Eq. (6) is associated with electron-phonon interaction and as such is an intrinsic property of InSb. The obtained magnitude and temperature dependence of τ_φ is in a good agreement with that obtained in Ref. [2].

The inelastic relaxation time τ_c is assumed to be independent on temperature. In our samples it is in the range $\tau_c = (1 \text{ to } 7) \times 10^{-12} \text{ s}$. We suppose that it is associated with extended structural defects of InSb thin films, such as the grain boundaries. In this model the conductivity electrons are dephased by inelastic scatterings from electrons occupying the interface states, which have a nonvanishing density of states at the Fermi level. In such a model τ_c can be related to the grain size L_c by $\tau_c \sim L_c^2/D$ (D the diffusion constant). For the obtained values of τ_c one obtains $L_c \simeq 100 \text{ nm}$. This is a magnitude of correct order in our samples.

It should be mentioned that our dependence $\tau_\varphi(T)$ resembles that found by Lin and Kao³⁸ for a large group of disordered polycrystalline metals. It is clear that our samples fall into this category. An interesting finding of Lin and Kao is also that many disordered metals have the same saturation dephasing length of about 100 nm. This value coincide with the value of our L_c . The sat-

uration observed in the temperature dependence of the dephasing time has been recently interpreted in terms of dynamical two-level systems associated with structural defects such as interfaces, dislocations, etc. These novel sources of dephasing are thought to be intrinsic to all samples with structural disorder. The obtained by us result $\tau_i = T^{-3}$ is in disagreement with that of Ref. [4] where a dependence of the type $\tau_i = T^{-2}$ has been found.

The postulated temperature dependence of τ_φ (solid lines in Fig. 4) was successfully used for the interpretation of the temperature dependence of the sample resistance above 2 K (Fig. 5). At lower temperatures, the temperature dependence of the resistance can be explained by the electron-electron interaction. We wish to draw attention to the fact that in the localization regime we were able to interpret both the temperature dependence of the MR and the resistance with the help of the same temperature dependence of inelastic time τ_φ and of the other parameters. This strengthens the parameter determination because the two physical effects are different and they are described by different formulae.

ACKNOWLEDGEMENTS

We thank Dr. T. Cichorek and Dr. A. Marucha from the Laboratory of Low temperatures and Structural Investigations PAS in Wroclaw for performing the measurements below 2 K. One of authors (V.D.) is thankful to the Institute of Physics of the Poznań Technical University for kind hospitality and to B. L. Altshuler for discussing several points of this work during the Localization'99 conference. This work was supported by P.P. Grant BW 62-184 and partly by INTAS Grant 2000-0476 and by NATO fellowship grant CP(UN)06/B/2001/PO.

* E-mail: maciej.oszwardowski@put.poznan.pl

¹ Y. Ootuka and A. Kawabata, *Progr. Theor. Phys. Suppl.* **84**, 249 (1985).

² R. C. Dynes, T. H. Geballe, G. W. Hull, and J. P. Garno, *Phys. Rev. B* **27**, 5188 (1983).

³ S. Morita, Y. Isawa, T. Fukase, S. Ishida, Y. Koike, Y. Takeuti, and N. Mikoshiba, *Phys. Rev. B* **25**, 5570 (1982); S. Morita, N. Mikoshiba, Y. Koike, T. Fukase, and S. Ishida, *J. Phys. Soc. Jpn.* **53**, 324 (1984).

⁴ R. G. Mani, L. Ghemin, and J. B. Choi, *Solid State Commun.* **79**, 693 (1991); *Phys. Rev. B* **43** 12630 (1991).

⁵ B. A. Aronzon, N. K. Chumakov, T. Dietl, and I. Wrobel, *Zh. Exper. Theor. Fiz.* **105**, 405 (1994) [*Sov. Phys. JETP* **78**, 216 (1994)]; B. A. Aronzon and N. K. Chumakov, *Physica B* **194-196**, 1167 (1994).

⁶ B. L. Altshuler, A. G. Aronov, D. E. Khmel'nitskii, and

A. I. Larkin, in *Quantum Theory of Solids*, edited by I. M. Lifshits (Mir, Moscow, 1982), pp. 130-237.

⁷ P. A. Lee and T. V. Ramakrishnan, *Rev. Mod. Phys.* **57**, 287 (1985).

⁸ B. L. Altshuler and A. G. Aronov, *Electron-Electron Interaction in Disordered Systems*, edited by A. L. Efros and M. Pollak (Elsevier, Amsterdam, 1985).

⁹ G. Bergmann, *Phys. Rep.* **107**, 1 (1984).

¹⁰ B. L. Altshuler, A. G. Aronov, A. I. Larkin, and D. E. Khmel'nitskii, *Zh. Eksp. Teor. Fiz.* **81**, 768 (1981) [*Sov. Phys. JETP* **54**, 411 (1981)].

¹¹ P. A. Lee and T. V. Ramakrishnan, *Phys. Rev. B* **26**, 4009 (1982).

¹² S. Maekawa and H. Fukuyama, *J. Phys. Soc. Jpn.* **51**, 3262 (1982).

¹³ Y. Isawa, K. Hoshino, and H. Fukuyama, *J. Phys. Soc. Jpn.* **51**, 3262 (1982).

¹⁴ A. Zawadowski, J. von Delft, and D. C. Ralph, *Phys. Rev. Lett.* **83**, 2632 (1999).

¹⁵ T. Berus, J. Goc, M. Nowak, M. Oszwardowski, and M. Zimpel, *Thin Solid Films* **111**, 351 (1984).

¹⁶ H. H. Wieder, *J. Vac. Sci. Technol.* **8**, 210 (1971).

¹⁷ M. Oszwardowski and T. Berus, *J. Phys. Chem. Sol.* **61**, 875 (2000).

¹⁸ M. Oszwardowski, T. Berus, and V. K. Dugaev, *Molecular Phys. Reports* **21** 139 (1998).

¹⁹ J. Kolodziejczak, *Acta Phys. Polon.* **20**, 289 (1961).

²⁰ E. M. Gershenzon, I. N. Kurilenko, L. B. Litvak-Gorskaya, and R. I. Rabinovich, *Fiz. Tekhn. Poluprov.* **7**, 1501 (1973) [*Sov. Phys. Semiconductors* **7**, 1005 (1974)].

²¹ C. Herring, *J. Appl. Phys.* **31**, 1939 (1960).

²² Yu. Kagan and A. P. Zhernov, *Zh. Eksp. Teor. Fiz.* **50**, 1107 (1966) [*Sov. Phys. JETP* **23**, 737 (1967)].

²³ W. Zawadzki and W. Szymanska, *Phys. Status Solidi B* **45**, 415 (1971).

²⁴ A. A. Abrikosov and L. P. Gorkov, *Zh. Exp. Teor. Fiz.* **42**, 1088 (1962) [*Sov. Phys. JETP* **15**, 752 (1962)].

²⁵ N. Papanicolaou, N. Stefanou, P. H. Dederichs, S. Geier and G. Bergmann, *Phys. Rev. Lett.* **69**, 2110 (1992).

²⁶ A. Kawabata, *Solid State Commun.* **34**, 431 (1980); *J. Phys. Soc. Jpn.* **49**, 628 (1980).

²⁷ S. Wang and P. E. Lindelof, *J. Low Temp. Phys.* **71**, 403 (1988).

²⁸ Y. Isawa, *J. Phys. Soc. Jpn.* **53**, 37 (1984).

²⁹ A. I. Larkin, *Pis'ma Zh. Exp. Teor. Fiz.* **31**, 239 (1980) [*JETP Letters* **31**, 220 (1980)].

³⁰ S. Kobayashi and F. Komori, *Prog. Theor. Phys. Suppl.* No. 84, 224 (1985).

³¹ B. L. Altshuler and A. G. Aronov, *Solid State Commun.* **38**, 1031 (1981).

³² J. Rammer and A. Schmid, *Phys. Rev. B* **34**, 1352 (1986).

³³ M. Yu. Reizer, *Phys. Rev. B* **40**, 5411 (1989).

³⁴ K. K. Larsen, M. van Hove, A. Lauwers, R. A. Donaton, K. Maex, and M. van Rossum, *Phys. Rev. B* **50**, 14200 (1994).

³⁵ V. V. Popov and V. V. Kasarev, *Phys. Status Solidi A* **58**, 231 (1980).

³⁶ M. Oszwardowski, T. Berus, and V. K. Dugaev. *Ann. Phys. (Leipzig)*, **8**, 201 (1999).

³⁷ P. Mohanty, E. M. Q. Jariwala, and R. A. Webb, *Phys.*

- Rev. Lett. **78**, 3366 (1997); P. Mohanty and R. A. Webb, Phys. Rev. B **55**, R13452 (1997).
- ³⁸ J. J. Lin and L. Y. Kao, J. Phys. Cond. Matter **13**, L119 (2001).
- ³⁹ B. L. Altshuler, M. E. Gershenson, and I. L. Aleiner, Physica E **3**, 58 (1998); I. L. Aleiner, B. L. Altshuler, Y. M. Galperin, Phys. Rev. B **63**, 201401(R) (2001).
- ⁴⁰ D. S. Golubev and A. D. Zaikin, Phys. Rev. Lett. **81**, 1074 (1998); cond-mat/0103166 (2001).
- ⁴¹ M. Büttiker, cond-mat/0106149 (2001).
- ⁴² Y. Imry, H. Fukuyama, and P. Schwab, Europhys. Lett. **47**, 608 (1999).
- ⁴³ B. Landolt-Börnstein. *Numerical Data and Functional Relationships in Science and Technology*, Vol. 22 (Springer, Berlin, 1987).

No	$d, \mu\text{m}$	$\mu, \text{cm}^2/\text{V}\cdot\text{s}$	$n \times 10^{-16} \text{cm}^{-3}$	$l = v_F\tau, \text{nm}$	$1/k_F l$	$r_s = 1/a_B k_F$	B_c, T	l_φ, nm
732	2.1	1080 (3500)	1.6 (1.6)	5.5 (18)	2.3 (0.72)	0.19 (0.19)	21.3 (2.0)	34 (62)
727	2.1	760 (830)	50 (15)	12 (9)	0.34 (0.68)	0.06 (0.09)	4.4 (8.2)	90 (64)
725	1.6	2770 (3000)	13 (1.9)	27 (16)	0.25 (0.75)	0.10 (0.18)	0.9 (2.5)	106 (61)

TABLE I. Electrical properties of the InSb<Pb> films at 4.2 K and calculated localization theory parameters. In the parentheses are given the data obtained from the curve fitting.

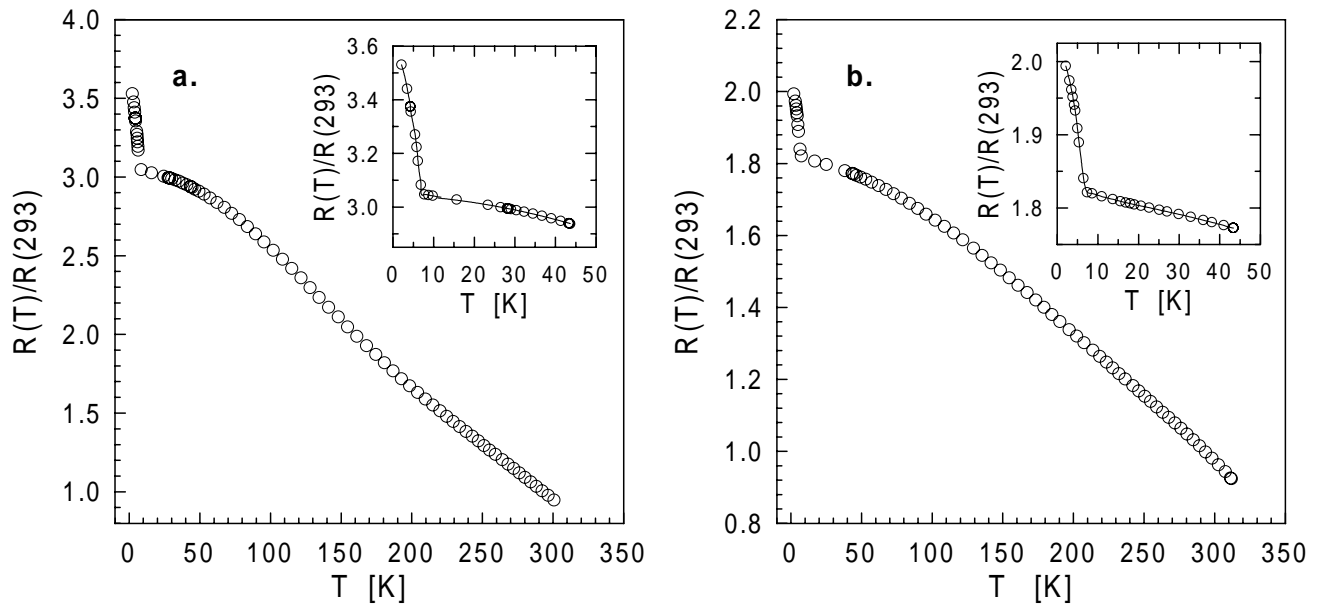


FIG. 1. The temperature dependence of relative resistivity of InSb<Pb> films below room temperature. (a) Sample 725B. (b) Sample 727. In the inserts the sharp increase in resistivity ascribed to the weak localization effect is presented in more details.

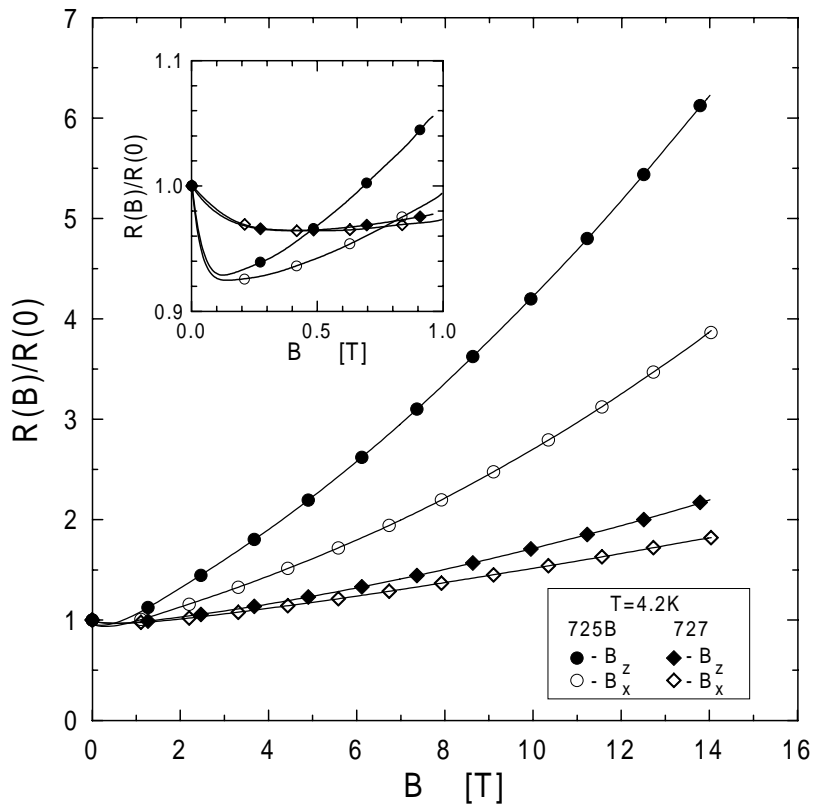


FIG. 2. The magnetic field dependence of the magnetoresistivity of samples 725B and 727 at 4.2 K. B_z and B_x are the directions of magnetic field towards the sample. At B_z the transversal MR is measured and at B_x the longitudinal MR is measured.

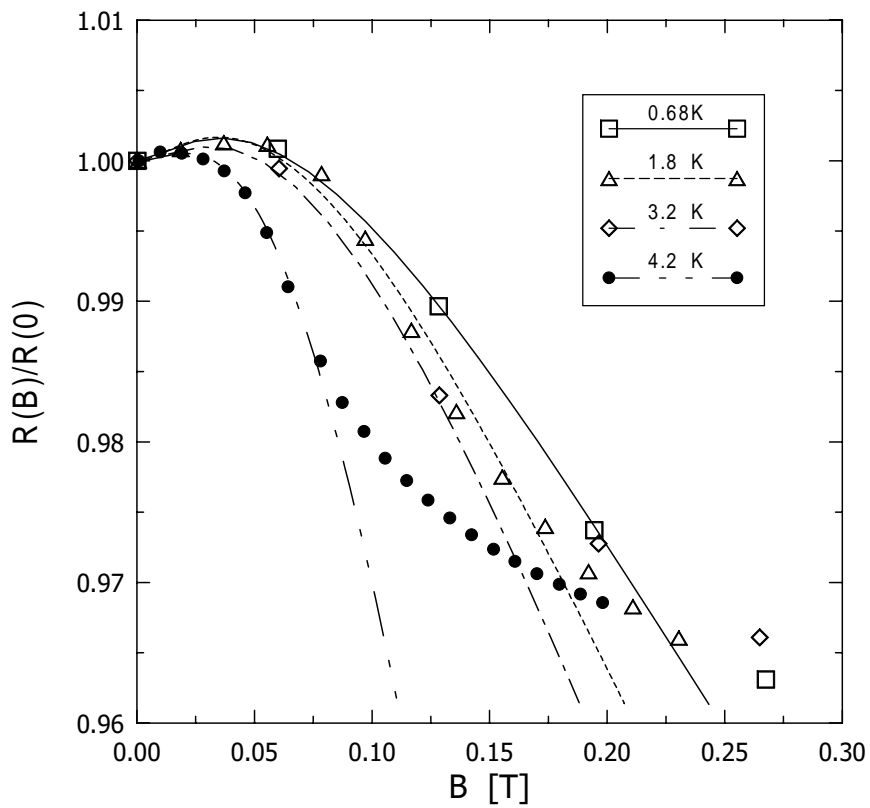


FIG. 3. Low field magnetoresistivity of sample 727 at various temperatures. The curves are fittings of the WL theory to the experimental points.

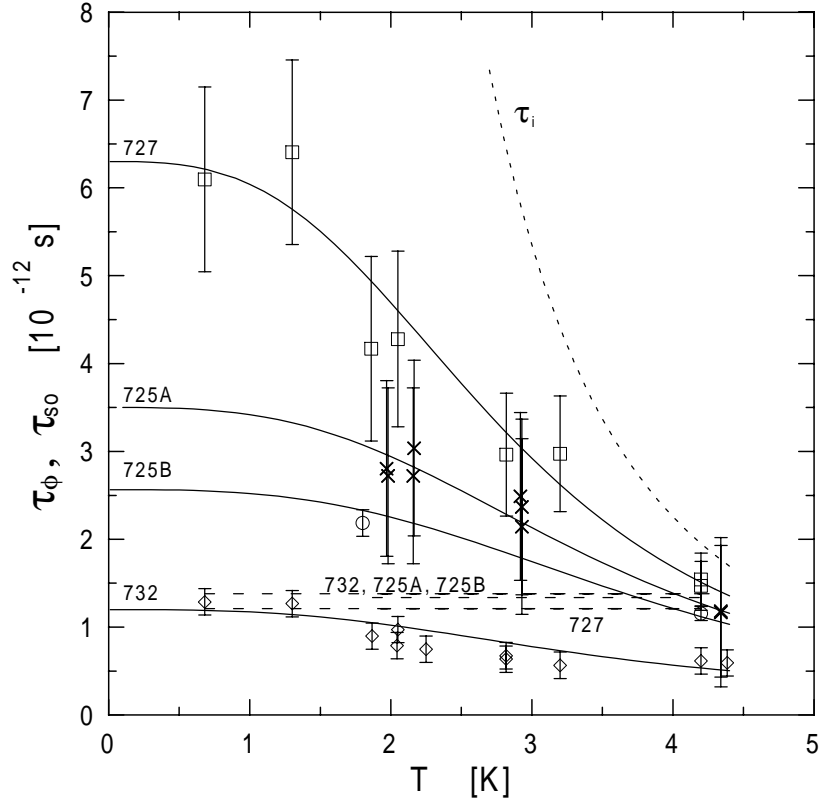


FIG. 4. Temperature dependencies of the inelastic relaxation times for samples 725A, 725B, 727 and 732 as obtained from the theoretical curve fittings to the experimental MR data. The solid curves are the values of τ_ϕ calculated from Eq. (5), the dashed lines are the values of τ_{so} , and the dotted line describes τ_i calculated from Eq. (6).

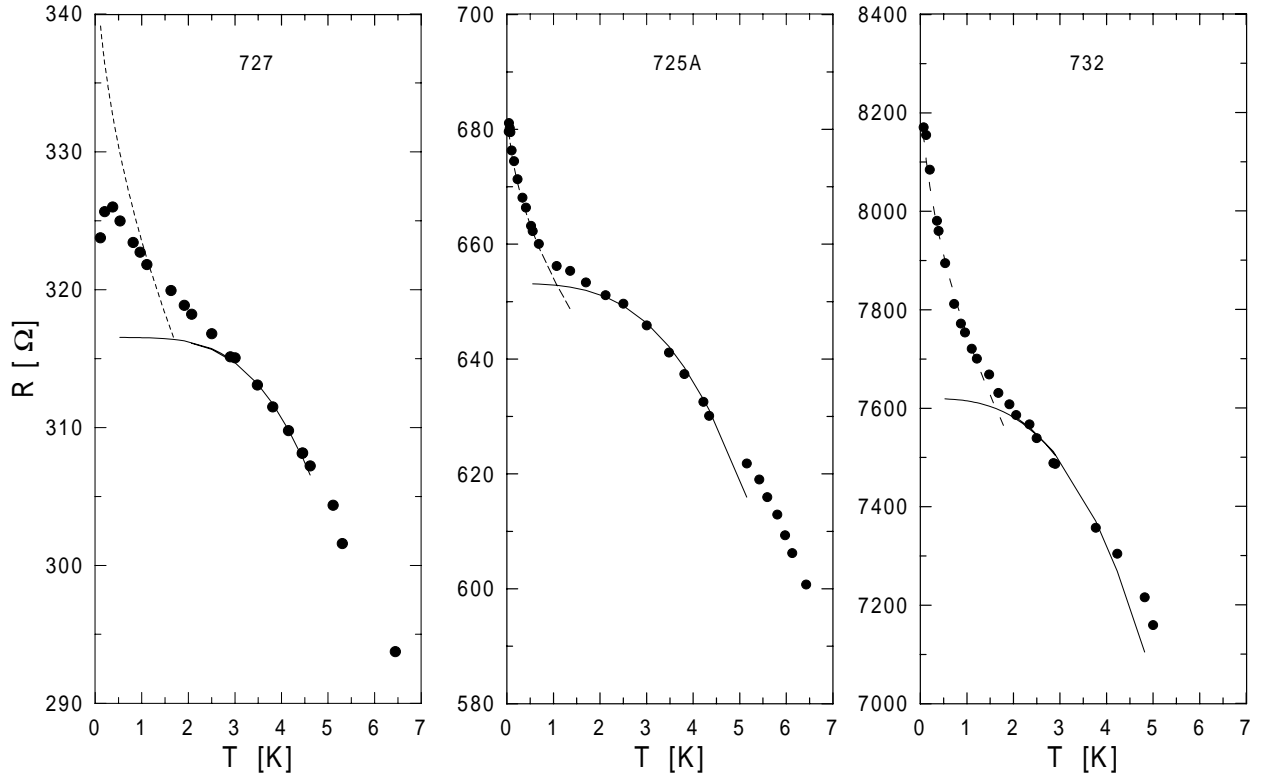


FIG. 5. The temperature dependence of resistance of samples 727, 725 and 732 between 40 mK and 7 K. The solid lines are calculated from Eqs. (8) and (9) as explained in the text.